NO_x-Abatement Potential of Lean-Premixed GT Combustors

T. Sattelmayer
Technical University Munich,
D-85748 Garching, Germany

W. Polifke

D. Winkler

K. Döbbeling

ABB Corporate Research,
CH-5405 Baden-Dättwil, Switzerland

The influence of the structure of perfectly premixed flames on NO_x formation is investigated theoretically. Since a network of reaction kinetics modules and model flames is used for this purpose, the results obtained are independent of specific burner geometries. Calculations are presented for a mixture temperature of 630 K, an adiabatic flame temperature of 1840 K, and 1 and 15 bars combustor pressure. In particular, the following effects are studied separately from each other:

- *molecular diffusion of temperature and species*
- *flame strain*
- *local quench in highly strained flames and subsequent reignition*
- *turbulent diffusion (no preferential diffusion)*
- *small scale mixing (stirring) in the flame front*

Either no relevant influence or an increase in NO_x production over that of the one-dimensional laminar flame is found. As a consequence, besides the improvement of mixing quality, a future target for the development of low-NO_x burners is to avoid excessive turbulent stirring in the flame front. Turbulent flames that exhibit locally and instantaneously near laminar structures ("flamelets") appear to be optimal. Using the same methodology, the scope of the investigation is extended to lean–lean staging, since a higher NO_x-abatement potential can be expected in principle. As long as the chemical reactions of the second stage take place in the boundary between the fresh mixture of the second stage and the combustion products from upstream, no advantage can be expected from lean–lean staging. Only if the primary burner exhibits much poorer mixing than the second stage can lean–lean staging be beneficial. In contrast, if full mixing between the two stages prior to afterburning can be achieved (lean-mix-lean technique), the combustor outlet temperature can in principle be increased somewhat without NO penalty. However, the complexity of such a system with a larger flame tube area to be cooled will increase the reaction zone temperatures, so that the full advantage cannot be realized in an engine. Of greater technical relevance is the potential of a lean-mix-lean combustion system within an improved thermodynamic cycle. A reheat process with sequential combustion is perfectly suited for this purpose, since, first, the required low inlet temperature of the second stage is automatically generated after partial expansion in the high pressure turbine, second, the efficiency of the thermodynamic cycle has its maximum and, third, high exhaust temperatures are generated, which can drive a powerful Rankine cycle. The higher thermodynamic efficiency of this technique leads to an additional drop in NO_x emissions per power produced.

Introduction

Due to its outstanding NO_x abatement potential, lean-premixed combustion has become the prevailing combustion technique of gas-fired land-based gas turbines within the last decade. Furthermore, progress has been made recently in the extension of the fuel spectrum toward liquid fuels as well as syngas from gasification processes. Since at high air pressures and temperatures lean premixing exhibits inherent flashback problems, compromises in regard to mixing quality had to be made until now in the design of reliable gas turbine burners, which result in elevated NO_x levels. However, improvements of the fuel–air mixing technique will lead to gas turbine burners that are free of these shortcomings in the near future. As a consequence, it becomes increasingly important to investigate how far the NO_x production of lean, perfectly premixed turbulent flames can be lowered.

The minimum attainable level for the unstaged process is influenced by the interaction of turbulence with chemistry. Modeling this interaction in sufficient depth would require a direct numerical simulation with detailed chemistry in order to capture the important influences on NO_x formation. Such numerical simulations up to now have been restricted to very simple flows and low turbulent Reynolds numbers. The computation of flows with a higher technical relevance, like combustor flows in our case, requires turbulence modeling and other crude simplifications with respect to the chemical reaction, so that the generation of a detailed understanding of the underlying phenomena cannot be expected.

Fortunately, the influence of turbulence-chemistry interaction on NO_x formation can be studied in sufficient detail as long as the minimum NO_x level is of technical interest. Since the local characteristics of premixed flames can be characterized by similarity numbers, a phenomenological description of effects that potentially may govern the NO_x formation can be given and the phenomena can be explored on the basis of model flames and reactor models, which are accessible for a full numerical modeling without excessive difficulty. This approach not only provides information about the NO formation of a turbulent flame front but, in addition, reveals the potential of lean and staged combustion methods.

The nitrogen chemistry as such is well enough understood for present purposes. As long as only clean fuels without fuel-

Contributed by the International Gas Turbine Institute and presented at Turbo Asia '96, Jakarta, Indonesia, November 5–7, 1996. Manuscript received at ASME Headquarters July 1996. Associate Technical Editor: J. W. Shinn. Paper No. 96-TA-21.

bound nitrogen are considered, three NO_x-formation paths, i.e., the so-called Zel'dovich, nitrous oxide (N_2O), and prompt mechanisms, contribute to the formation of NO in lean premixed combustion. The prompt mechanism, based on available rate data, exerts a negligible-to-weak effect in high pressure, lean flames. For the flame zone of atmospheric, lean, premixed combustors, the mechanism can be significant and has to be considered. As the excess air and/or the pressure increases, the ratio of NO formed by the Zel'dovich mechanism to NO formed by the nitrous oxide mechanism decreases. This is due to the high activation energy of the Zel'dovich mechanism and the pressure sensitivity of the N_2O formation. Under the conditions of greatest interest for gas turbine combustion, namely near lean extinction and at high pressures, the nitrous oxide mechanism is predominant and can account for essentially all of the NO formed [1]. Since the NO formation through all three paths strongly depends on the concentration of the radicals of the oxyhydrogen pool, the NO is formed mainly in the flame zone, where superequilibrium concentrations are observed. Farther downstream, after the breakdown of the fuel and the consumption of the intermediates is completed, the NO production drops to the rate given by the Zel'dovich mechanism at O-equilibrium. As a consequence, for primary zone temperatures below approximately 1750 K no significant dependence of the NO_x emissions on the combustor residence time is found.

Although some differences in the NO_x-formation rates predicted from different reaction mechanisms are found in the literature, only the results computed on the basis of the mechanism for methane proposed by Miller and Bowman [2] will be presented throughout the paper. It is important to note that the findings presented subsequently were not altered qualitatively when using different models. Combustion process parameters are chosen to represent current development targets for utility heavy-duty gas turbines.

Flame Structures of Gas Turbine Burners

Turbulent processes in flames are characterised by a broad range of time and length scales. In swirling flows, the size of the largest vortices with the turbulent macroscale L_t is strongly linked to the burner size. Perturbations with long wavelengths generate large vortices, which subsequently interact with each other and form a cascade of smaller and smaller vortices of increasing frequency [3]. The turbulent kinetic energy, which is mainly concentrated in the motion of the large vortices, is finally dissipated at vortex sizes below the Kolmogorov scale.

In order to characterize the interaction between turbulence and chemistry, similarity parameters can be defined. The governing parameters can be grouped within a set of essentially five dimensionless numbers. The ratio u'/s_l and the ratio L_t/δ_l relate properties of the large-scale turbulence to parameters that characterize a one-dimensional laminar flame. In addition, the turbulent Reynolds number Re_t relates the transport by large turbulent vortices (''turbulent diffusion'') to molecular transport (diffusion), whereas the Damköhler number Da compares

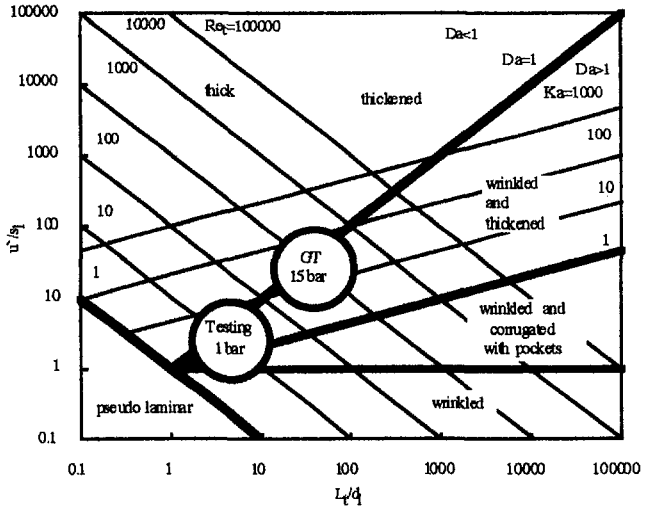

Fig. 1 Turbulent combustion diagram

the mixing time due to the large-scale vortex motion to the characteristic chemical time scale of a laminar one-dimensional flame. The Karlovitz number Ka relates this chemical time scale to the mixing time of the smallest vortices in the turbulent energy cascade. Different definitions for Ka are found in the literature based either on the Taylor scale λ or on the Kolmogorov microscale η and with a variety of constants proposed. Interestingly, the Karlovitz number is also a measure for the volumetric heat release, since it relates the chemical time scale of the flame front to the generation of flame surface in the turbulent case. Implicitly, in defining the Damköhler number and the Karlovitz number, it is assumed that the mixing time within turbulent eddies correlates well with the time for eddy rotation. This might not be fully justified at least for low turbulent Reynolds numbers [4]. The five parameters mentioned are not independent from each other but can be coupled via the relationships of the turbulent cascade of isotropic turbulence. (A summary of the most important relationships as well as the aforementioned definitions are listed in Appendix A). When the turbulent Reynolds number Re_t, the Damköhler number Da, and the Karlovitz number Ka are expressed as a function of u'/s_l and L_t/δ_l, turbulent flames can be characterized in the so called Borghi diagram [5] (Fig. 1).

The two marked spots in the diagram represent the conditions for typical premixed gas turbine burners in an engine and at atmospheric test conditions, respectively. The highest Karlovitz numbers appear at the maximum air preheat and represent operating points near the lean blowout limit (the burner rating is 5–10 MW thermal output at 15 bar combustor pressure, turbulent length scales were obtained by LDA measurements, and the laminar flame speed and flame thickness were computed with a one-dimensional premixed flame model).

Nomenclature

a = thermal diffusivity, m^2/s
a = strain rate, s^{-1}
A = area, m^2
D = diffusion coefficient (species), m^2/s
Da = Damköhler number
Da_{mix} = mixing Damköhler number = τ_{mix}/τ_{chem}
ϵ = turbulent dissipation rate, m^2/s^3
δ_l = laminar flame thickness, m
η = Kolmogorov scale, m
k = turbulent kinetic energy, m^2/s^2
Ka = Karlovitz number
L_t = turbulent macroscale, m
Le = Lewis number = a/D
λ = Taylor scale, m
λ = thermal conductivity, W/m/K
ν = kinematic viscosity, m^2/s
p = pressure, N/m^2
Re_t = turbulent Reynolds number
s_l = laminar flame speed, m/s
t = time, s
$t_{burnout}$ = burnout time (99.9 percent reaction progress), s
t_{res} = residence time, s
T = local temperature, K
T_{ad} = adiabatic flame temperature, K
T_{in} = reactant temperature at inlet, K
τ = characteristic time scale, s
u' = rms of turbulent fluctuations, m/s
X = mole fraction

A set of borderlines can be defined, where turbulent flames change their appearance due to changes in the interaction of turbulence with chemistry. However, since the methodology depends on the comparison of two phenomena competing with each other with subsequent neglecting of the influences of the weaker partner as well as on the validity of relationships of isotropic turbulence, a sharp transition cannot be expected when such a borderline is crossed. Turbulent premixed flames have been a major research field for a long time and many detailed investigations of particular effects present in turbulent flames have been published. Subsequently, a brief overview of the current knowledge will be given. In interpreting the results from the review, an attempt is made to develop an understanding of the phenomena governing the structure of turbulent flames with respect to the properties of the underlying flow field. The following flame types can be defined.

"Pseudo" Laminar Flames. In flows with local laminar flame structure, the turbulent Reynolds number of all possible vortex sizes must be less than unity. This condition is satisfied if $\mathrm{Re}_t < 1$. Since the viscous dissipation is strong in comparison with the turbulent transport, this leads to immediate dissipation, so that the character of the flame is well represented by the relationships of a one-dimensional laminar flame.

Wrinkled Flames. Reacting flows with low turbulence intensity and turbulent length scales, which are considerably greater than the thickness of the flame front, generate a wrinkling of the reactive layer with an increase in total flame area and volumetric heat release. As long as u' remains smaller than the laminar flame speed s_l, the flame front exhibits a connected surface.

Wrinkled, Corrugated Flames With Pockets. Turbulent structures with intensities u' above the laminar flame speed s_l cause a disruption of the flame surface. Zones of high velocity can, for example, bend the local flame zone so strongly that locally Ω-shaped bulges of products are generated and finally separated from the main flame front (pockets) after the reaction at the link to the main flame front has been quenched.

Flames of the three aforementioned types have been subject to a large number of detailed investigations. Although the global appearance of the flame front is strongly influenced by turbulence, it is commonly understood that with respect to NO production no major deviations from the mechanisms found in one-dimensional flames can be expected. As long as the laminar flame is faster than the turbulent velocity u' and the flame is much thinner than the size of all turbulent eddies, it can be concluded that the combustion process is locally well represented by the laminar flame theory. In comparison to this so-called (unstrained) flamelet regime, the current understanding of premixed, highly turbulent flames is much less consistent. Stirring of the flame front by turbulent eddies, the increase of the diffusion due to turbulence as well as the local stretching of flame fronts during flame–vortex interaction with subsequent quenching and re-ignition may affect the NO production of premixed flames.

Thickened, Wrinkled Flames. As soon as the Karlovitz number exceeds unity, the dissipation of turbulent kinetic energy will require a drop in the turnover time of the smallest eddies below the reaction time of the laminar flame front. It is postulated in the literature [6] that the smallest eddies of the turbulent flow field will produce stirring in the reacting layer and will alter the appearance of the flame front. The turbulent scales smaller than the flame thickness produce a thickening of the reactive layer due to enhanced (turbulent) diffusion of temperature and species, whereas the larger scales wrinkle the thickened flame front. The increase in heat release is attributed to the generation of flame area (wrinkling) as well as to an increase of flame speed. It is important to keep in mind that the mixing process in the flame front, which finally leads to thickening, is generated by the rotational motion of vortices. Since this kind of stirring produces continuously backward and forward mixing, it leads to the mixing of media with different levels of reaction progress during the combustion process. It has to be expected that the relationship between the concentration of radicals governing NO formation and the average reaction progress is altered with respect to the laminar case. It is somewhat unclear presently how quickly flame thickening occurs when the Karlovitz number is increased above unity.

Thickened (Thick) Flames. Increasing the Karlovitz number further shifts the critical vortex size, which separates the regime of flame thickening from that of flame wrinkling, toward the largest vortices of the turbulent flow field ($\mathrm{Da} = 1$). Above that limit ($\mathrm{Da} < 1$) even the turnover time of the largest vortices is shorter than the chemical time scale. As a consequence, the wrinkled flame structure is lost entirely and the flame front appears as a thick reacting layer, which progresses with high turbulent flame speed. The reacting layer between reactants and products can be interpreted as an ensemble of stirred spots with a wide range of sizes, which promote the diffusion of temperature and species. The continuous transition (time average) from reactants to products implies directly that the characteristic size of the stirred spots does not exceed the thickness of the reaction zone. A widely used classical model of a highly stirred flame is the perfectly stirred reactor (PSR). However, the PSR does not fulfill the constraint that the characteristic size of the stirred spots does not exceed the thickness of the reaction zone because the homogeneous reaction volume cannot be subdivided in areas of different time-averaged reaction progress. Since the homogeneous reaction volume is obtained at the expense of a discontinuity at the inlet of the reactor, fundamental differences between the reaction in highly turbulent flames and stirred reactors exist.

Stretched Flames. Besides flame front stirring and enhanced diffusion due to turbulence, flame stretch might alter the radical pool during reaction. As already mentioned, the ensemble of turbulent vortices produces fluctuating strain to which the flame front is exposed while it propagates against the flow direction. A flame is locally stretched when in a frame of reference moving with the flame the velocity normal to the flame front undergoes deceleration toward the reaction zone. At the same time, a velocity component parallel to the flame front develops. In contrast to the unstrained one-dimensional flame, which consumes all the reactants it has previously preheated, the strained flame is characterized by a continuous convective loss of reactants during preheat. Flame zones of high strain are found, e.g., where a counterflow from opposite sides toward a point of stagnation occurs [7]. The case of a counterflow of reactants from one side and products from the second side is of particular interest for strained premixed flames. At very low strain rates the flame front is located far from the stagnation point. The velocity gradient is low when compared to the flame thickness and no fundamental difference is found with respect to laminar flames. At high strain rates, however, the reaction zone is remarkably influenced by the convective/diffusive transport of products and temperature toward the flame front from the side beyond the stagnation point. Strain increases the gradients of species and temperature and, as a consequence, diffusive fluxes. Near the point of stagnation itself the transport is dominated by diffusion alone. The combined diffusion and convection of products and temperature toward the reactive layer leads to an enhanced heating and a dilution of the reactants with products.

The NO concentration is composed of one contribution that originates from the reaction and a second share that is transported with the counterflowing products toward the reactive layer. This makes the comparison of the NO emissions from strained and unstrained flames difficult. A special procedure

described in Appendix B can be used to separate the NO generated in the flame from the amount that originates from the product side.

The disturbance of the balance between the heat release and the diffusion as well as the convection of temperature and species alters the flame front characteristics considerably. The generation of strain can be accomplished by vortices of all sizes. Since vortices at the lower end of the turbulent energy cascade produce the highest strain (see Appendix A), a Karlovitz number on the order of unity, the so-called Klimov–Williams limit, is of special interest. On the other hand, the interaction time of the smallest vortices might be insufficient to influence the flame strongly enough. A number of investigations [7–11], which cover the more generic case of single vortices and assume that a superposition of effects from different vortex sizes is permissible, consistently predict a limit for local quenching at Karlovitz numbers above unity. An efficiency function can be calculated that takes into account that the smallest vortices cannot maintain flame stretch long enough. The interesting result that vortices of a medium size in between the turbulent microscale and macroscale are most effective is found (valid for flames with $L_t/\delta_l > 5-10$).

Re-ignition and Afterburning. In highly strained flames, a certain share of the reactants cannot react immediately despite the existence of an interface between reactants and products. The understanding of this phenomenon, how complete combustion is finally achieved, is not very well developed yet. Usually, the description that subsequent reaction takes place in "distributed reaction zones" is found in the literature without detailed definition.

The enhanced convective/diffusive fluxes in strained zones lead to a velocity component parallel to the flame front and a loss of matter sideways. Counterflows of reactants and products with high strain rates are characterized by huge convective/diffusive fluxes with respect to the heat release in the flame front. Asymptotically, a pure mixing process is approached for infinite strain rates. It is important to mention that, although the temperature and species concentration change due to chemical reaction might be negligible for excessive strain rates, a breakdown of the combustion process does not occur for a counterflow of reactants and products. As the result of the mixing process, a wide range of mixture ratios of reactants and products are generated, which will undergo an afterburning process in zones of lower local strain. As long as no temperature increase due to diffusion takes place, zones of high reactant concentration will either assume temperatures below the self-ignition limit, or temperatures that require long induction times for the onset of chemical reaction. In contrast, zones of higher product concentration will exhibit a higher temperature in the adiabatic case. A massive drop of the local strain rate will directly lead to a smaller ratio between convective/diffusive fluxes and heat release. Thus, structures similar to those of an unstrained flame will appear and "re-ignition" will mainly progress via the diffusion of temperature and species from the hotter zones toward the zones of higher reactant content. Although it is somewhat unclear whether the self-ignition of isolated pockets of mixtures is of evidence in addition, a model that assumes "the distributed reaction zones" to be a local sudden combustion without any diffusive transport is certainly unrealistic. If one assumes that the formation of flame fronts, which propagate diffusion-driven into a mixture of reactants and products, represents the reality more adequately, the (unstrained or weakly strained) combustion of mixtures of reactants and products, a kind of local exhaust gas recirculation, can be defined as a simplified model for the afterburning process. A model can be constructed that depicts highly turbulent flames as an ensemble of highly strained flame zones complemented by weakly strained zones of combusting reactant/product mixtures. However, the transition toward the highly stirred (thick) flame regime or the well-stirred reactor can not be described adequately as long as stirring caused by the turbulent eddies is excluded.

In general it has to be mentioned that detailed investigations on stretched flames reported in the literature were restricted to the generic case of single vortices. Effects due to the coexistence of vortices of different sizes were not covered. So, stirring effects by smaller vortex sizes were beyond the scope of those investigations. Furthermore, local flame quenching was not easy to monitor experimentally or needed crude assumptions like massive radiative heat loss in order to become visible in numerical investigations.

In summary, the current knowledge does not provide a full understanding for Karlovitz numbers above unity. Besides known effects like flame stretch and afterburning in distributed reaction zones, turbulent mixing in the flame front has to be considered in order to generate a consistent understanding of the structure of turbulent flames over a wide range of turbulence intensities and length scales.

Modeling the Effect of Turbulence on NO Generation. Figure 1 reveals that the flame structure of gas turbine burners cannot be universally characterized by one single turbulent flame regime. Burners operated very close to lean extinction (1650–1750 K) are represented by Karlovitz numbers between 10 and 100 and Damköhler numbers near unity, whereas an increase of the flame temperature toward 1900–2000 K will reduce the Karlovitz number remarkably. In terms of the turbulent flame structure, it has to be expected that this will be accompanied by a change from a highly stirred and stretched flame toward flamelet structures. In order to assess whether turbulence affects the NO emissions of perfectly premixed flames from gas turbine combustors, a number of simplified models will be defined.

The reference case is the one-dimensional laminar flame, which represents not only the laminar but also the moderately turbulent (unstrained flamelet) regime. The computations of the freely propagating flames presented in this paper are accomplished by the widely used Sandia codes [12]. NO formation in laminar flames is influenced by the diffusion of species. Diffusion is complex, since each species has its own individual diffusion coefficient, which depends on all other species and on the temperature field.

A model that is widely used in NO studies is the combination of a stirred reactor and a plug flow reactor. Although the flame stabilization of turbulent flames due to the diffusion of temperature and species is not well represented by a PSR, the combination PSR–PFR is useful when the PSR volume is minimized. The need for the PSR as an "artificial" ignition zone, which compensates for the missing flame holding capability of the PFR, does not constrain too severely the investigation of NO formation, which happens mainly in the mid and high-temperature regime. Usually, only small amounts of NO are produced at the exit of the PSR and the further formation can be studied in the absence of diffusive transport.

Turbulent diffusion, which is in reality generated by vortex motion, is often strongly simplified for the purpose of flow modeling. The transport term is modeled largely similar to the laminar case, with the major difference that the diffusion coefficient depends on turbulent quantities of the flow field and is no longer species or temperature dependent. Thickening of flame fronts due to turbulence enhanced diffusion can be studied using the laminar flame code when the matrix of the diffusion coefficients is replaced by one "turbulent" value and the strength of the transport of temperature with respect to the transport of species is predetermined by the selection of the Lewis number Le. In order to compute the one-dimensional flame with turbulent diffusion coefficients, the laminar flame code was modified accordingly. The benefit of this model is threefold: First, the influence of turbulent diffusion, which is usually at least an order of magnitude higher than in the laminar

case, can be studied and, second, the impact of preferential diffusion of species on NO formation can be quantified. Third, the sensitivity of the NO production on the balance between the diffusion of temperature and the diffusion of species can be quantified, if the Lewis number is varied. It can be shown analytically from the underlying equations that the propagation velocity of the flame as well as the flame thickness δ are both proportional to the square root of the diffusivity of temperature and species and, as a consequence, the reaction progress with respect to time is *not* a function of the diffusivity. In other words, the local turbulence level and the turbulent macroscale will influence the flame propagation and the volumetric heat release but not the time scale of the chemical reaction and not the formation of NO. A particle that crosses the flame front will not experience any difference when the diffusion coefficients a and D are similarly scaled (i.e., to maintain a constant Lewis number).

The representation of the turbulent interactions with the flame by turbulent diffusion has the shortfall that the character of stirring by vortex motion, namely to mix media of different reaction progress continuously in the flame front, is not accounted for. A number of advanced models have been proposed in the past that account for stirring (e.g., "Interaction by Exchange with the Mean" model [13], "Coalescence-Dispersion" model [14, 15]). Simply speaking, in these models the flow volume under consideration is divided into a number of subvolumes ("particles") with homogeneous mixture in each of them. The mixture in each subvolume reacts according to a full kinetics scheme. The particles travel randomly from the inlet of the apparatus to the exit and interact with each other according to the assumptions of the particular model. The results obtained generally deliver NO emissions below those computed for a PSR as an upper limit. Flame stabilization in such models without diffusive transport requires backmixing of "older" to "younger" material when the incoming mixture is too cold to undergo self-ignition. Although promising agreement with reactor experiments has been obtained, it appears to be difficult to specify the model constants and assumptions so that turbulent flame fronts are well represented. Hence, for our purpose we restrict the investigation to the classical PSR–PFR combination mentioned above and vary the PSR volume in order to account for stirring. It is worth mentioning that the PSR is an extreme (asymptotic) assumption for the modeling of the turbulent stirring in a flame front. The intense stirring, which is enabled by the existence of the reactor confinement and high velocities, is generally not achieved in propagating flames as long as the burner pressure loss is, as usual, only a small fraction of the system pressure. Therefore, the PSR will overpredict effects on NO formation considerably.

A flame front that propagates in a turbulent flow field is continuously exposed to fluctuating strain produced by turbulent eddies. Using the code of Rogg [16, 17] for a counterflow flame, the influence of flame stretch on NO formation is calculated. The study focuses on the counterflow of premixed reactants and products since this is more relevant for highly turbulent flames than the counterflow of reactants on both sides.

In order to assess the importance of afterburning in zones that have previously undergone mixing without significant heat release due to locally high strain rates, the one-dimensional unstrained laminar flame of mixtures of reactants and products has been additionally investigated. At higher product concentration in the mixture, the self-ignition temperature is exceeded and the well-known problem of defining the cold boundary arises. This difficulty has been overcome in calculating a burner-stabilized flame instead of a freely propagating one. In increasing the flow rate toward the point of liftoff the heat loss to the "burner" was almost fully suppressed and adiabatic conditions were established. For the sake of simplicity, the products mixed with the reactants were free of NO. As far as lean combustion is concerned, it can easily be shown that the NO content of the primary mixture does not influence the NO generation of the afterburning process and that no significant reburning of the NO from the first combustion will happen during afterburning. As a consequence, the NO production of the afterburning can be separated from that of the primary process and a superposition is allowed.

Results for the Unstaged Flame

Laminar flame propagation is governed by the diffusion of temperature (heat conduction) from the hot products toward the cold reactants. The boundary between the preheat zone, which absorbs more heat than it generates, and the reaction zone is located near the turning point of the temperature curve. At 1 bar (Fig. 2) heat release starts at approximately 25 percent temperature rise (900 K) and peaks at approximately 70 percent. In addition to heat conduction, the diffusion of species influences the appearance of the flame front considerably. For example, the fuel concentration has dropped to approximately 50 percent of the initial value due to diffusion before the heat release starts, and at the point of maximum heat release the fuel has already been fully converted to intermediates. Diffusion also widens the area where intermediates like CO are found and transports products toward zones of low temperature. Increasing the pressure to gas turbine conditions leads to significant changes. As the thermal conductivity λ is independent of pressure, the thermal diffusivity $a = \lambda/(c_p\rho)$ is inversely proportional to the pressure p. Due to the higher thermal capacity of the reactants with increasing pressure, the transport of temperature is slowed down and the reaction rate is increased. Both effects generate steeper gradients in the flame front and the flame becomes thinner and slower. The heat release is

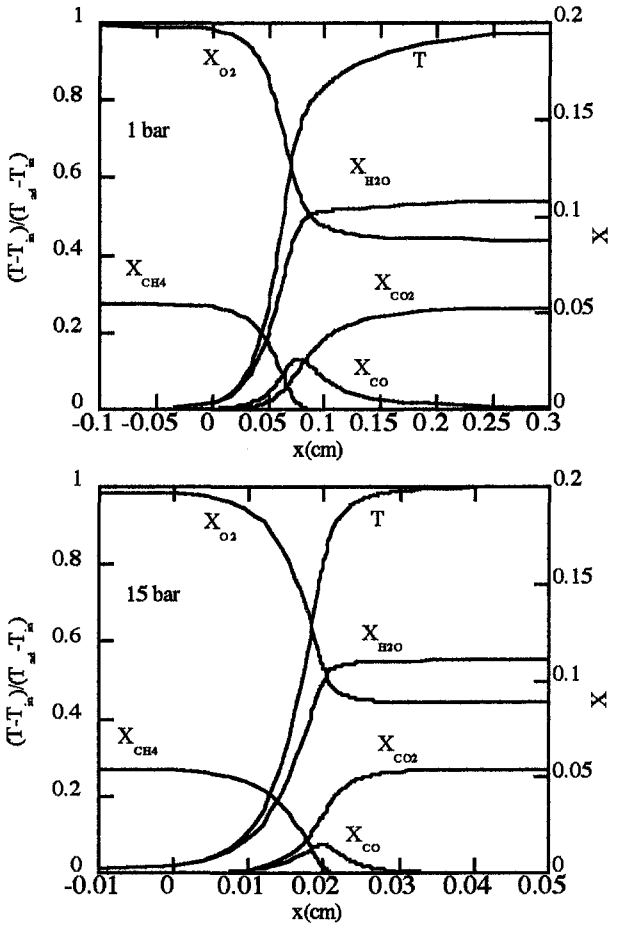

Fig. 2 Pressure effects on laminar flame fronts

shifted toward higher temperatures and peaks at 85 percent temperature rise (15 bar).

In order to demonstrate the dependence of important species, key radicals, the NO concentration, and the NO production rate from temperature, a reaction progress variable $(T_{ad} - T)/(T_{ad} - T_{in})$ is introduced (Fig. 3), which describes the temperature deficit with respect to the final state T_{ad} (1 = reactant temperature T_{in}, 0 = adiabatic flame temperature T_{ad}). As long as the prompt NO formation is of minor importance, an assessment of the NO formation can be made solely on the basis of the O, H, and OH radical concentrations with respect to temperature (and a characteristic reaction time). Since it can be shown for all cases under consideration that OH as well as H concentrations are closely linked to the O radical, only the latter will be presented in the graphs as a measure for the generation of NO in the flame. With increasing pressure, the recombination of radicals is enhanced and the O radical concentration drops. The pressure sensitivity of the NO formation paths as well as the altered diffusion lead to higher NO concentrations at low temperatures. The comparison of the NO mole fraction and the NO production rate reveals that the NO concentrations seen at low temperatures are due to diffusion from downstream (Fig. 3). At high pressure, the NO production rate is negative below 40 percent reaction progress due to the shift of NO to NO_2. This high-pressure effect is responsible for the undesired formation of yellow smoke from gas turbine combustors at low load. Fortunately, the NO_2 is fully converted back to NO in the high-temperature regime of adiabatic premixed flames.

At first, the missing pressure influence on the NO concentration appears surprising for the adiabatic flame temperature under

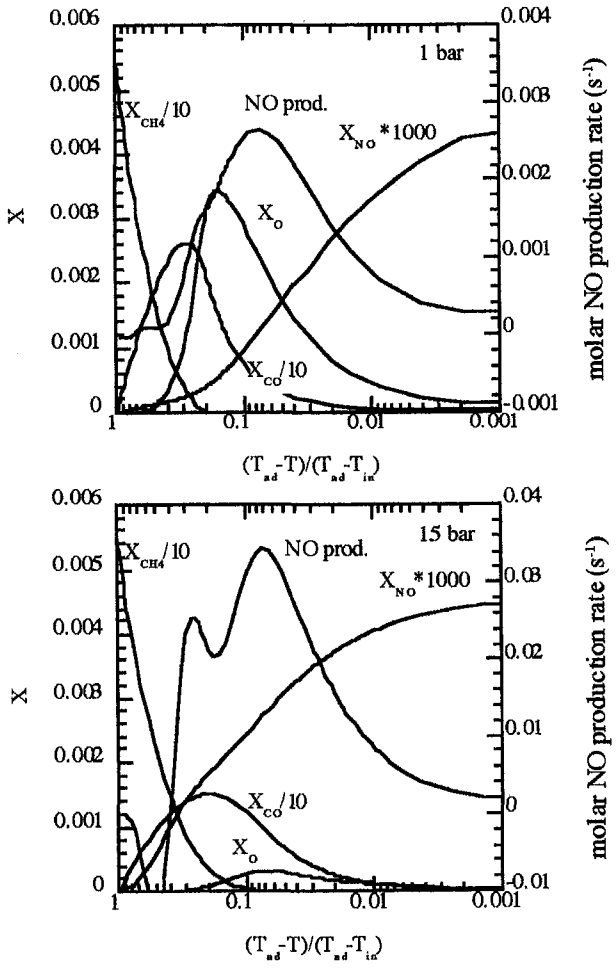

Fig. 3 NO formation in laminar flame fronts

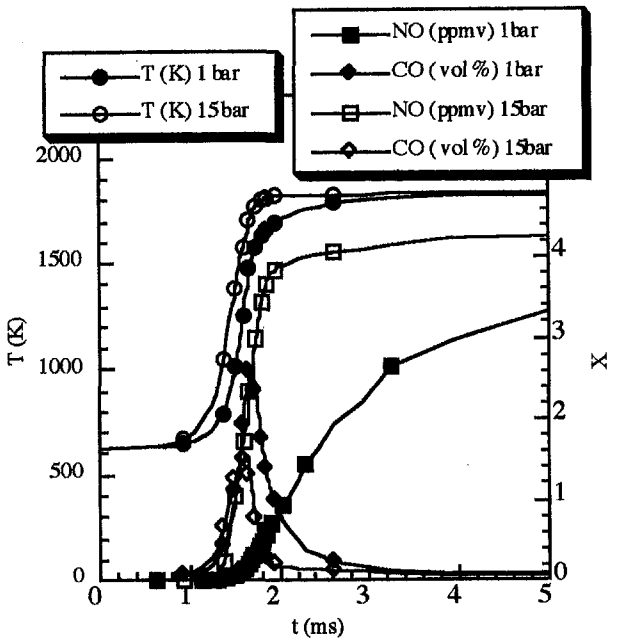

Fig. 4 Pressure influence on reaction progress of laminar flame fronts

consideration (1840 K), which is beyond the threshold of the pressure-sensitive thermal NO formation. At higher T_{ad}, the NO concentration at 99.9 percent reaction progress even drops when the pressure is increased. As Fig. 4 shows, the reaction becomes much shorter at high pressure. A comparison of the two cases for the same residence time would reveal a considerably higher NO level for the high-pressure case. If the burnout time at 1 bar is selected for the comparison (e.g., 99.9 percent reaction progress), this corresponds to holding the high-pressure case for a long time after burnout at T_{ad}. Even at the equilibrium concentration of the O radical, the pressure-dependent thermal NO formation route produces significant additional postflame NO.

Diffusion influences the relationship between key radicals and temperature, e.g., the diffusive radical transport into hotter zones enhances the NO formation. The effects can be quantified, if combustion is accomplished in the diffusion-free environment of a plug flow reactor PFR. At 1 bar, the PSR at incipient extinction provides 70 percent of reaction progress and heat release (Fig. 5). It is easy to understand that radical concentrations at the PSR exit are higher when compared to the laminar flame, since a higher share of the chemically bound energy has been released already. Although only 30 percent of the heat is released in the PFR, the radical concentrations quickly progress toward the values found in the laminar flame front. The lower slope of the NO curve is due to the quicker reaction progress, which reaches approximately twice the speed of the laminar case. This acceleration is caused by the fact that the temperature rise in the PFR is not damped by the diffusive heat loss toward the preheat zones. The lower NO concentrations of the PSR–PFR combination with respect to the laminar case were found similarly for both pressures and the whole range of flame temperatures investigated ($T_{ad} < 2000$ K). In summary, it can be concluded that the somewhat unphysical absence of the diffusive transport did not change the NO emissions more than a change in adiabatic flame temperature of 20–60 K.

The transition from the laminar flame to a flame with "turbulent" gradient diffusion leads to a relative reduction of the diffusion of the lighter species with respect to those with a higher molecular weight. As shown in Fig. 6 for a Lewis number of unity, the peak concentration of the NO-generating O radical is higher than in the laminar case. The same applies to the H

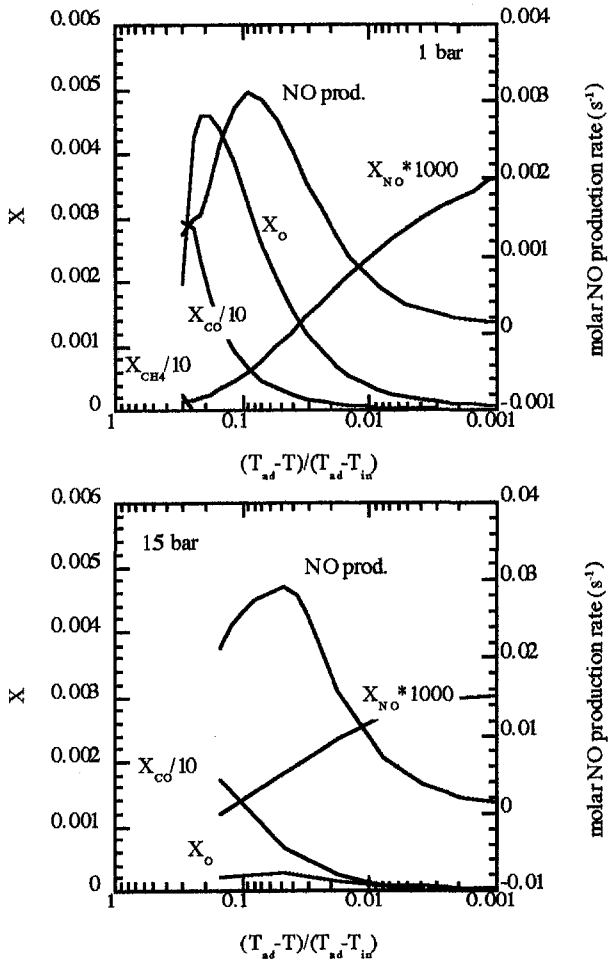

Fig. 5 NO formation of a PSR–PFR combination

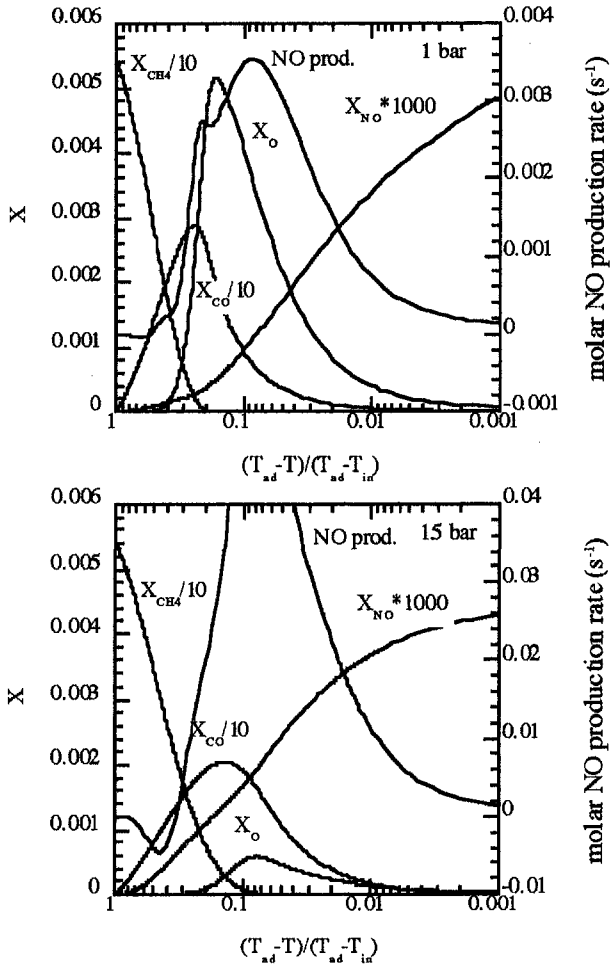

Fig. 6 NO formation of a one-dimensional flame with "turbulent" diffusion

radical (not shown here). In spite of the higher radical concentration, the final NO level is not considerably altered. This has to be attributed to the drop in reaction time, which goes along with the transition to the turbulent diffusion concept. It can be concluded that the preferential diffusion of the species in a laminar flame does not remarkably influence the NO generation.

A useful feature of the concept of turbulent diffusion is that the strength of species diffusion with respect to the diffusion of temperature can easily be altered. The case of high Lewis numbers (low species diffusion) is of particular interest, since the extent to which the propagation and reaction density of a premixed flame front depend on the diffusion of species can be studied. When the diffusion of fuel as well as of radicals is impeded, no significant radical attack from the reaction zone toward the preheat zone will take place. This results in a strong preheating of the reactants before the reaction is initiated. For Le = 5 and 1 bar, the heat release peaks at 1666 K (200 K higher than in the laminar case). The higher effective preheat temperature at the starting point of the reaction goes along with a stronger heat loss from the reaction zone. Due to the importance of the Zel'dovich mechanism at 1 bar, the NO emission is increased by approximately 30 percent. A similar effect is not found at 15 bar, since the N_2O mechanism, which dominates at high pressures, does not respond to the shift of the reaction toward higher temperatures in the same way. Increasing the species diffusion (Le = 0.07) will enhance the transport of fuel into the reaction zone strongly and all radical concentrations are much lower than in the other cases, whereas no significant effect on the NO levels was found. Figure 7 shows the heat release pattern of four cases, namely the laminar flame and the flame with turbulent diffusion and three different Lewis numbers (Le = 0.07, 1, 5). The global increase of species diffusion lowers the reaction progress considerably. Decreasing species diffusion results in a very quick heat release and a steep temperature rise. Effects of preferential diffusion of light species, which are an essential characteristics of laminar flames, lead to a less intense heat release than the Le = 1 case. The calculations reveal that the NO emission of one-dimensional flames exhibits

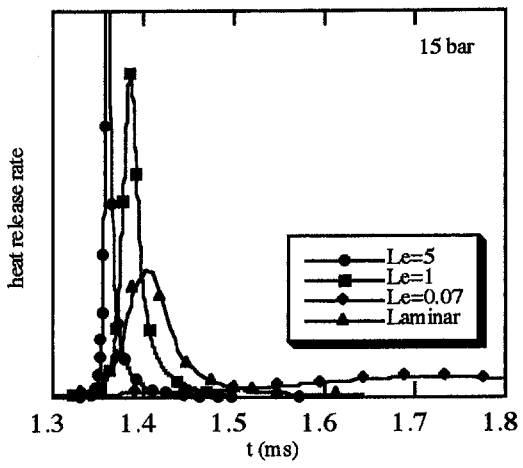

Fig. 7 Lewis number effects on one-dimensional flame fronts

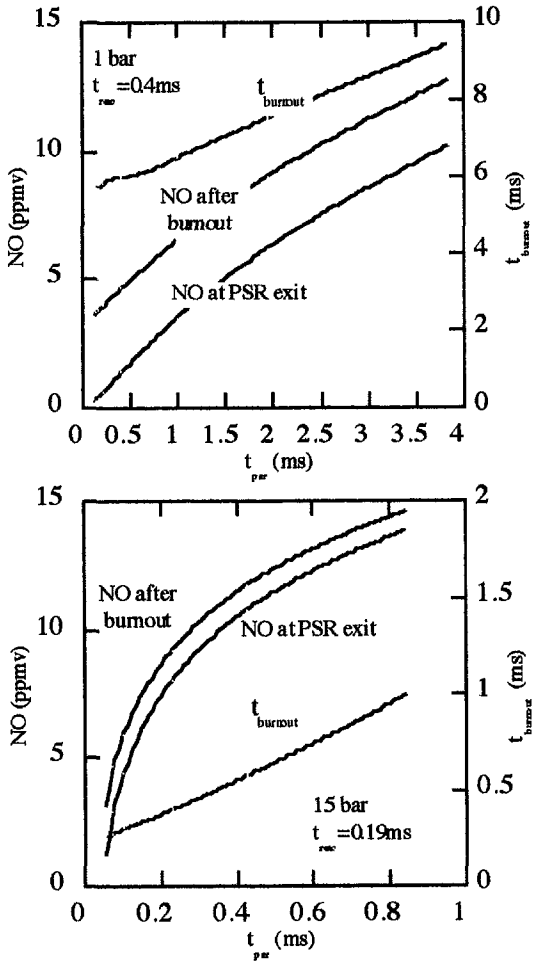

Fig. 8 Effect of stirring on the NO emission

a remarkably low sensitivity to even crude and unphysical manipulations of the diffusive transport.

As already mentioned, the goal of modeling the influence of turbulent eddies on the flame front realistically by a gradient formulation cannot be achieved, since the effect of stirring is not adequately represented. In order to obtain an estimate for the strength of the effect of stirring on NO, Fig. 8 presents the NO emissions (99.9 percent reaction progress) of the PSR–PFR combination and a wide range of residence times (PSR reactor volume). The comparison with the characteristic chemical time scale t_{reac}, which has been derived from the temperature profiles of the laminar flame, is of particular interest, since it allows one to assess in principle how strongly stirring can effect the NO formation. At 1 bar, changing the residence time in the PSR (below t_{reac}) will not substantially influence the NO emission, whereas the NO slope is steep at 15 bar. At 1 bar, as a consequence, in order for a major impact of stirring on NO formation to occur, a strongly overproportional thickening of the flame front with respect to the propagation velocity would be required, which cannot be seen in gas turbine burner investigations [18]. At high pressures, however, a significant impact of stirring on NO can be expected. Although it is difficult to draw quantitative conclusions from Fig. 8, the statement might be accepted for 15 bar, that the potential increase in the NO emission due to stirring is on the order of the NO emission of the unstirred flame.

An influence of strain on the NO emission of strained flames can be expected when the strain rate is of the order of the inverse of the reaction time. Computations were performed at 1 bar pressure and strain rates between 1000 1/s $< a <$ 10,000 1/s as well as at 15 bar pressure and strain rates between 2000 and 20,000 1/s. In Fig. 9 the NO concentrations are plotted over the reaction progress variable $(T_{ad} - T)/(T_{ad} - T_{in})$. A direct comparison of the NO generation in the strained case with the unstrained case cannot be immediately made, since a fixed value has to be set at the product inlet of the computational domain [17], which then influences the NO value at the right boundary $(T_{ad} - T)/(T_{ad} - T_{in}) = 0.001$ of Fig. 9. In the computations shown in Fig. 9 the NO concentrations of the corresponding unstrained flames (99.9 percent reaction progress) were specified for the NO concentration in the product stream.

The remarkable influence of the strain rate can only be seen at low pressures. When compared to the unstrained flames, higher NO concentrations are generally found at low temperatures. By virtue of the data reduction technique described in Appendix B, the mole fraction $X_{products}$ of the species, which originate from the product side, are calculated. For the highest strain rates a proportionality between $X_{products}$ and the reaction progress is approached (Fig. 10). Consequently, it can be concluded that at high strain rates, mixing of cold reactants and hot products have a strong impact on temperature changes due to chemical reaction. Since it is not observed that the volumetric heat release rate is influenced by strain (not shown here), the effect is caused by the increase of the convective/diffusive

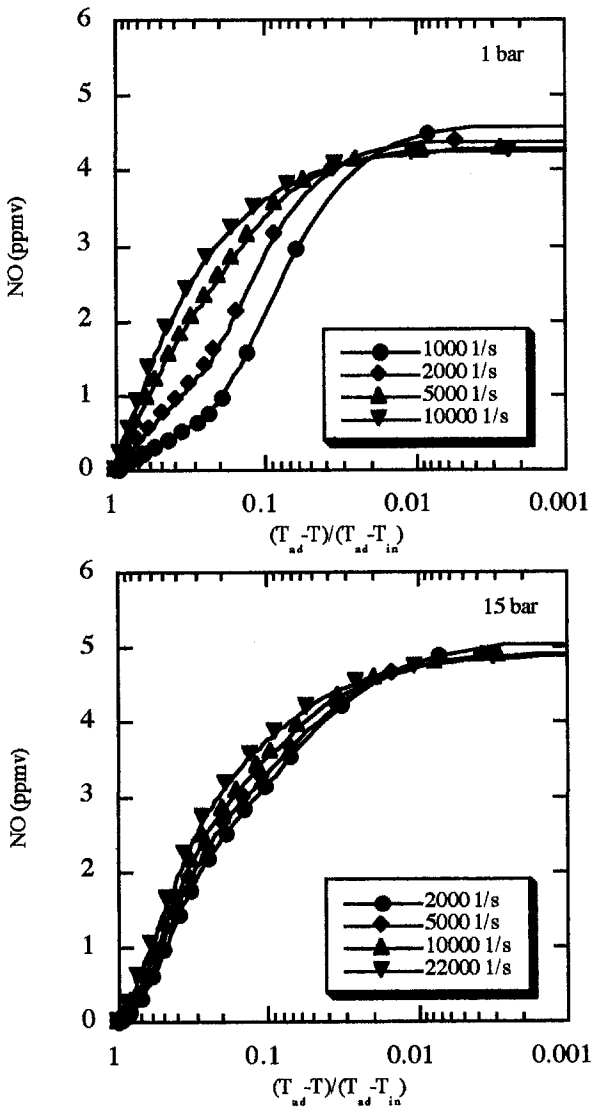

Fig. 9 NO concentration in strained flames

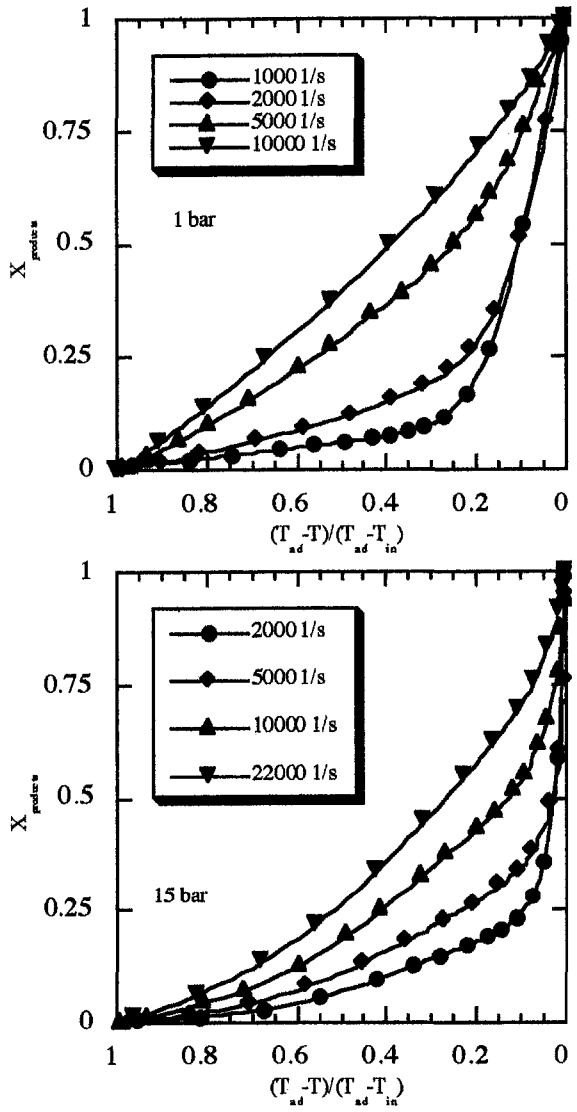

Fig. 10 Mixing of products with reactants in strained flames

fluxes at high strain rates. Interestingly, a sudden extinguishing of the flame (quench) is not observed, because the product side represents an infinite source of heat. Due to the decrease of the diffusivities a and D with pressure, the regime, where considerable "product" concentrations $X_{products}$ are found at low strain rates, is restricted at 15 bar to $(T_{ad} - T)/(T_{ad} - T_{in}) < 0.1$ (>90 percent reaction progress), whereas the influence is extended down to approximately 70 percent reaction progress at atmospheric pressure. After the separation of the NO, which originates from the product inlet, from the flame-generated NO (Appendix B), Fig. 11 is obtained. High flame stretch has an NO-reducing effect. The same results yields Fig. 12, where the NO-production rate is shown for comparison.

The distribution of strain rates in turbulent flows can be obtained on the basis of isotropic turbulence [3]. It can be shown that very high strain rates occur relatively seldom and that the global NO emission of a flame front is dominated by regimes exposed to low to medium strain. Consequently, it cannot be expected that the calculated effect of locally high strain on NO generation will remarkably reduce the NO emissions from gas turbine burners.

The flame zones with high local strain that generate unburned mixtures of reactants and products will undergo an afterburning process after the strain strength has been released. In Fig. 13 the results for the mixture temperature of 1273 K, which corresponds to a ratio of approximately unity of reactant mixture to product mixture, are presented. Surprisingly, the radical concentrations recover the level seen in the case of the combustion of pure reactants (Fig. 3) very quickly, despite the fact that the fuel concentration is lowered by 50 percent. NO emissions at 1 bar are also almost identical due to the Zel'dovich mechanism, which is characterized by the NO generation in the high-temperature regime of the reactive layer. Per quantity fuel, almost twice as much NO has been generated. In contrast, at high pressure a start of the afterburning at higher temperature reaction is beneficial due to the characteristics of the predominant N_2O path. With the assumption that the products, which are mixed with the reactants upstream of the flame, contain NO according to an unstrained flame ($=NO_{unstrained}$) at $(T_{ad} - T)/(T_{ad} - T_{in}) = 0.001$ (99.9 percent reaction progress), the results of a set of calculations with different ratios of reactants and products are summarized in Fig. 14. At 1 bar afterburning stimulates total NO formation clearly, whereas at 15 bar no net effect can be detected. In addition, Fig. 14 shows that the same result is found on the basis of a PSR-PFR/PFR model. It can be concluded that high local flame strain, which leads to lower NO,

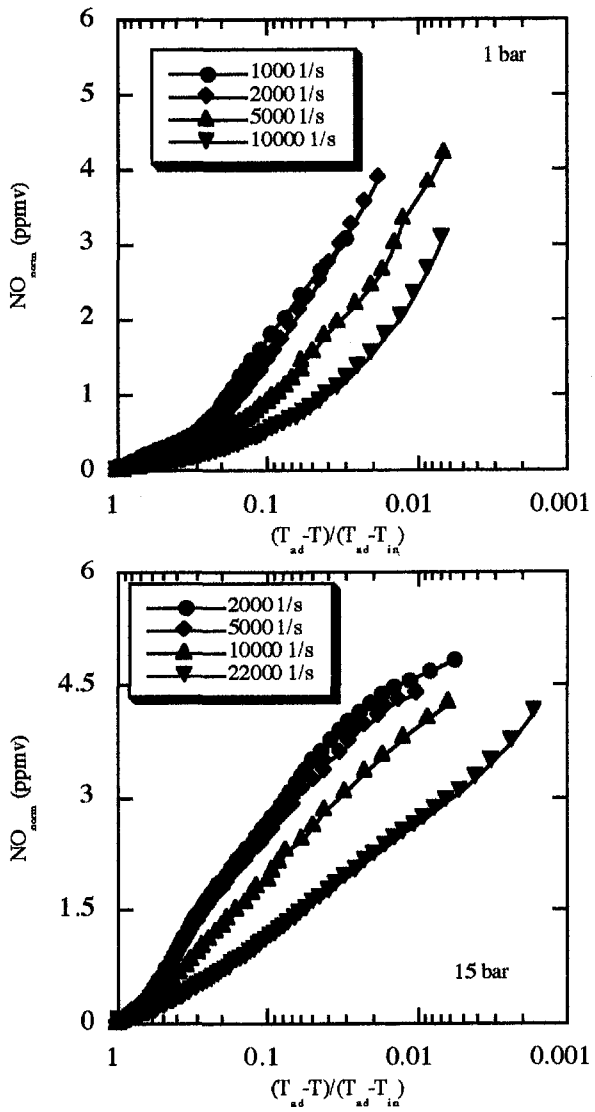

Fig. 11 Flame-generated NO in strained flames

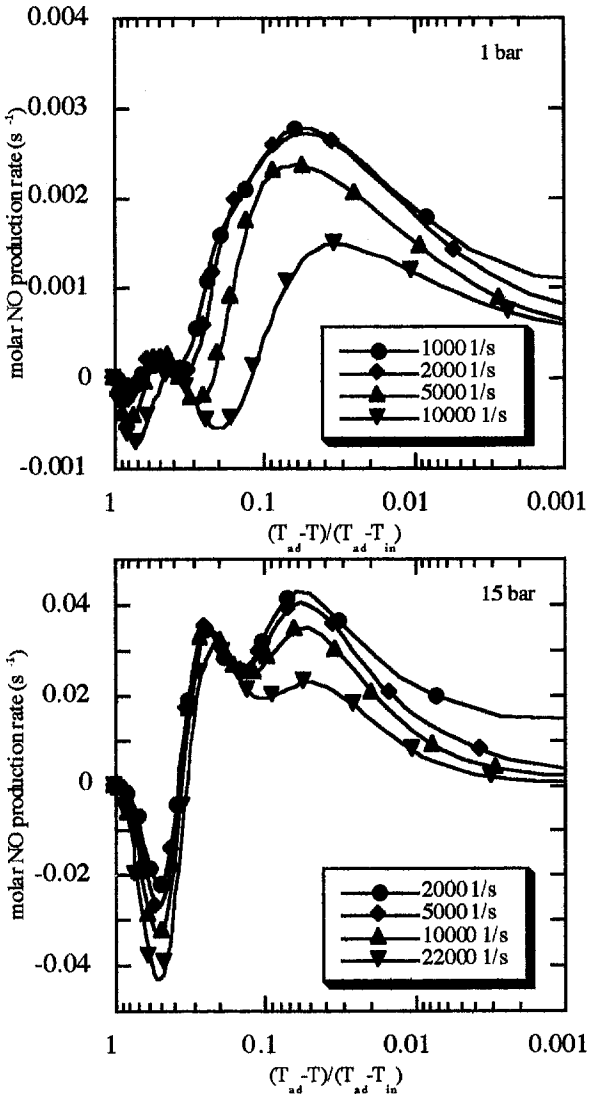

Fig. 12 NO production rate in strained flames

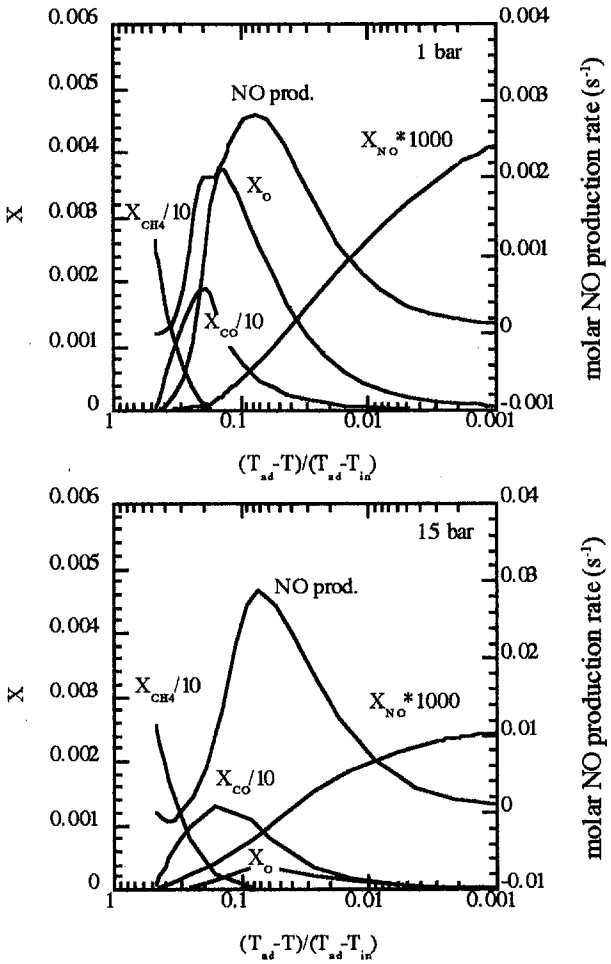

Fig. 13 NO from the unstrained combustion of a NO free mixture of products and reactants

is accompanied by an afterburning process of diluted reactants, which has an adverse effect on NO as long as the pressure is low.

Staging Effects

If the reactants of a second stage are fed into the exhaust of a first stage, which has previously approached the adiabatic flame temperature, no significant difference to the aforementioned effects in the unstaged flame is to be expected. The reactive layer between the media of both stages exhibits a structure according to the corresponding turbulent combustion regime. Of greater interest is the following scenario: In a first very lean (or catalytic) stage nearly NO-free exhaust gas is generated, which is diluted with air until the desired temperature is achieved. This temperature is selected low enough to permit enough mixing time for fuel injection in a second stage (or a richer fuel–air mixture) before the second ignition takes place. The final temperature (of 1840 K) is reached after the completion of the burnout of the secondary fuel. Figure 15 depicts the NO emissions of such a lean-mix-lean process. The mixing Damköhler number Da_{mix} has been derived from engine experience. Only in the region below unity can perfect fuel admixing be reached (mixing element size realistic for gas turbine application) before the reaction is initiated in the second stage. It is evident that at 1 bar even for NO free exhaust from a first stage no considerable benefit exists, whereas at 15 bar a reduction of NO by 50 percent seems to be the limit.

However, the assumption that no NO in the first stage is generated is unrealistic: For perfectly premixed, aerodynami-

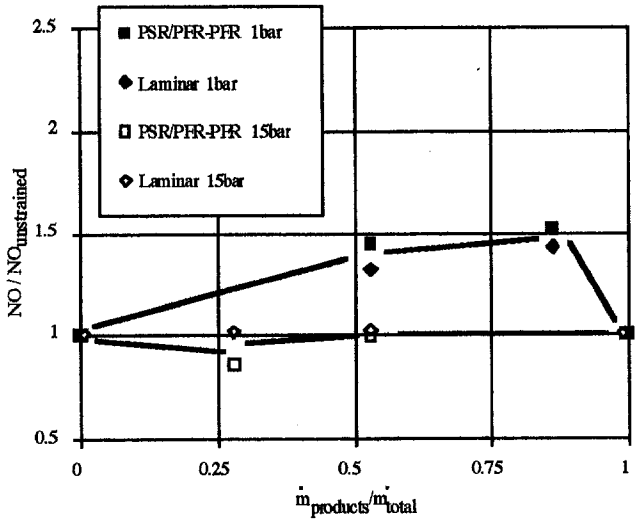

Fig. 14 Influence of afterburning on NO

cally stabilized flames, lean blowout temperatures below approximately 1700 K are difficult to achieve with sufficient blowout margin. Since this limits the NO concentration from the first stage to approximately 2 ppm (one-dimensional laminar flame results for 1700 K), the net effect of staging will be considerably smaller. It is questionable whether any advantage remains, when the larger liner surface of a staged system, which has to be cooled and reduces the air available for combustion, is taken into consideration. In contrast, the characteristics of lean-mix-lean systems match very well the requirements of modern gas turbine reheat cycles, which provide ideal inlet temperatures in the second stage due to the partial expansion in a high-pressure turbine after primary combustion. In these cases a reduction of NO is achieved primarily due to the higher thermodynamic efficiency. The ABB gas turbine family GT24/26 comprises the first implementation of this ultralow NO_x reheat principle.

Conclusions

The study of model flames with full chemistry reveals that the one-dimensional flame represents a good model for gas turbine burners at moderate turbulence levels. The NO abatement potential of a moderately turbulent combustor is shown in Fig. 16 (Miller and Bowman mechanism). The importance of residence time for high adiabatic flame temperatures is apparent. Residence times below 10 ms are difficult to achieve with current designs, since the mixing time exceeds by far the chemical time. Burners with a high number of small-scale elements offer a promising way to minimize residence time in the future.

Excessive stirring within the reactive layer of the flame enhances NO production and should be avoided in the design of high-pressure gas turbine burners.

Flame strain locally lowers NO formation. However, a strong influence on the emissions from burners cannot be expected because of the strain distributions found in turbulent flow fields.

Afterburning of previously "quenched" flame zones leads only at low pressures to higher NO formation.

The NO generation of premixed flames is remarkably insensitive to changes in the diffusive transport of temperature and species or the absence of diffusive transport.

Staged combustion will only have an influence on NO emissions when mixing between the stages occurs before the second reaction is initiated. The NO reduction potential is moderate and might be lost due to the bigger volume and higher complexity of a staged combustor.

Staged (sequential) lean–lean combustion is attractive for reheat cycles, since higher thermodynamic efficiencies can be achieved.

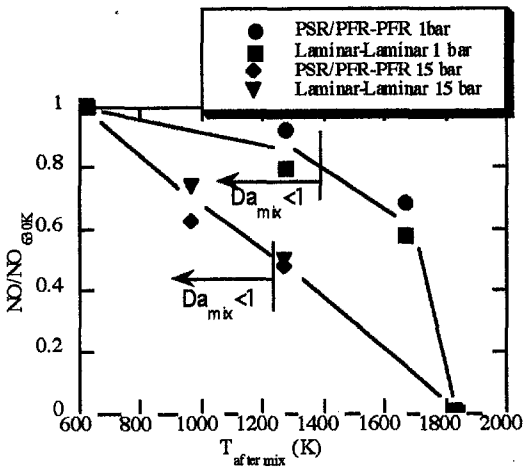

Fig. 15 NO emissions from a lean-mix-lean process

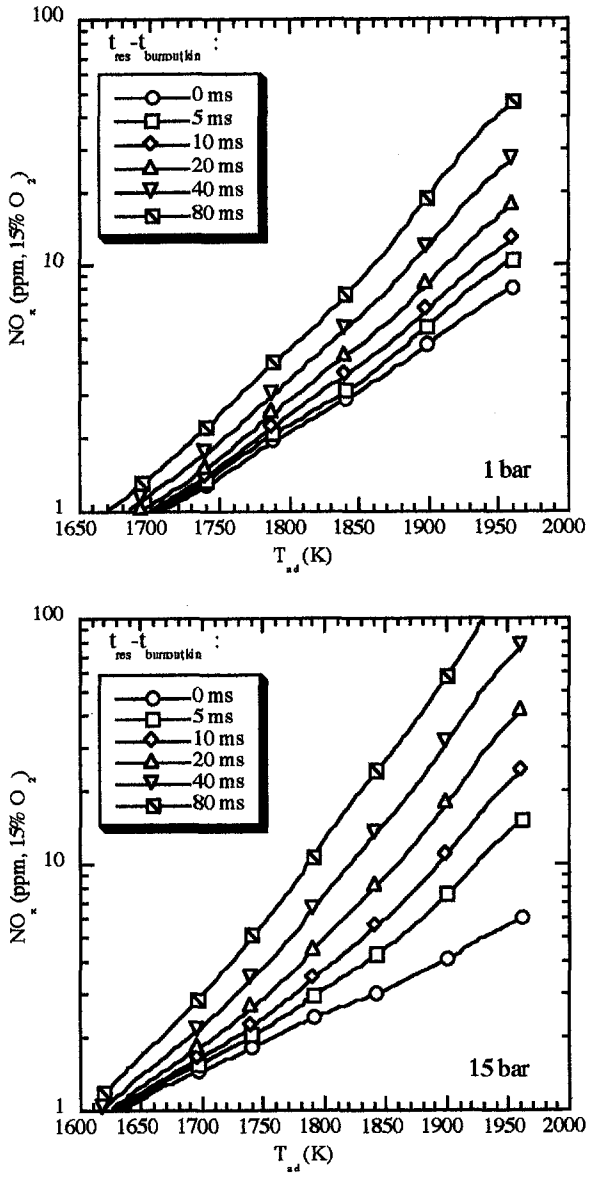

Fig. 16 NO abatement potential of kinetically controlled gas turbine combustors

References

1 Nicol, D. G., Steele, R. C., Marinov, N. M., and Malte, P. C., "The Importance of the Nitrous Oxide Pathway to NO_x in Lean-Premixed Combustion," ASME JOURNAL OF ENGINEERING FOR GAS TURBINES AND POWER, Vol. 117, 1995, pp. 100–111.

2 Miller, J. A., and Bowman, C. T., "Mechanisms and Modeling of Nitrogen Chemistry in Combustion," *Prog. Energy Combustion Sci.*, Vol. 15, 1989, pp. 287–338.

3 Tennekes, H., and Lumley, J. L., *A First Course in Turbulence*, MIT Press, 1985.

4 Koochesfaharni, M. M., and Dimotakis, P. E., "Mixing and Chemical Reactions in a Turbulent Mixing Layer," *LFM*, Vol. 170, 1986, pp. 83–112.

5 Borghi, R., "Turbulent Combustion Modeling," *Prog. Energy Combustion Sci.*, Vol. 14, 1988, pp. 245–292.

6 Zimont, V. L., "Theory of Turbulent Combustion of a Homogeneous Fuel Mixture at High Reynolds Numbers," *Combust. Expl. and Shock Waves*, 1979, pp. 305–311.

7 Meneveau, C., Poinsot, T., "Stretching and Quenching of Flamelets in Premixed Turbulent Combustion," *Combustion and Flame*, Vol. 86, 1991, pp. 311–332.

8 Poinsot, T., Veynante, D., and Candel, S., "Diagrams of Premixed Turbulent Combustion Based on Direct Simulation," *23rd Symp. (Int.) on Combustion*, 1993, pp. 613–619.

9 Roberts, W. L., Driscoll, J. F., Drake, M. C., and Goss, L. P., "Images of the Quenching of a Flame by a Vortex to Quantify Regimes of Turbulent Combustion," *Combustion and Flame*, Vol. 94, 1993, pp. 58–69.

10 Abdel Gayed, R. G., and Bradley, D., "Criteria for Turbulent Propagation Limits of Premixed Flames," *Combustion and Flame,* Vol. 62, 1985, pp. 61–68.
11 Abdel Gayed, R. G., and Bradley, D., "Combustion Regimes and the Straining of Turbulent Premixed Flames," *Combustion and Flame,* Vol. 76, 1989, pp. 213–218.
12 Kee, R. J., Grcar, J. F., Smooke, M. D., and Miller, J. A., "A Fortran Program for Modeling Steady Laminar One-Dimensional Premixed Flames (Chemkin Manual)," Sandia Report SAND85-8240, 1985.
13 Correa, S. M., "Turbulence-Chemistry Interactions in the Intermediate Regime of Premixed Combustion," *Combustion and Flame,* Vol. 93, 1993, pp. 41–60.
14 Curl, R. L., "Dispersed Phase Mixing: Theory and Effects in Simple Reactors," *AIChE J.,* Vol. 9, pp. 175–181.
15 Tonouchi, J. H., Pratt, D. T., "A Finite-Rate Macromixing, Finite-Rate Micromixing Model for Premixed Combustion," The Combustion Institute Fall Meeting, 1995, Stanford University, Paper 95F-167.
16 Rogg, B., "Response and Flamelet Structure of Stretched Premixed Methane–Air Flames," *Combustion and Flame,* Vol. 73, 1988, pp. 45–65.
17 Rogg, B., "RUN-1DL; The Cambridge Universal Laminar Flamelet Computer Code," *Reduced Kinetic Mechanisms for Applications in Combustion Systems,* Springer, 1993.
18 Kampmann, S., Leipertz, A., Döbbeling, K., Haumann, J., and Sattelmayer, T., "Two Dimensional Temperature Measurements in a Technical Combustor With Laser Rayleigh Scattering," *Applied Optics,* Vol. 32, No. 30, Oct. 1993, pp. 6167–6172.

APPENDIX A

Relationships of Isotropic Turbulence and Definitions

Inertial range (Kolmogorov):

$$\epsilon \propto \frac{u^3_{\text{vortex}}}{l_{\text{vortex}}} \propto \frac{l^2_{\text{vortex}}}{t^3_{\text{vortex}}} \propto \text{const}$$

Vortex characteristic velocity:

$$u_{\text{vortex}} \propto l^{1/3}_{\text{vortex}}$$

Vortex turnover time:

$$\tau_{\text{vortex}} \propto l^{2/3}_{\text{vortex}}$$

Strain rate:

$$\tau_{\text{vortex}} = \tau_s$$

$$a = \frac{1}{\tau_s} = \frac{dA_{\text{flame}}/dt}{A_{\text{flame}}} = \frac{u_{\text{vortex}}}{l_{\text{vortex}}} \propto 1/l^{2/3}_{\text{vortex}}$$

Macroscale:

$$L_t \propto \frac{u'^3}{\epsilon} \quad \tau_{L_t} \propto \frac{u'^2}{\epsilon} \approx \frac{k}{\epsilon}$$

Taylor scale:

$$\lambda \propto L_t/\text{Re}_t^{1/2} \propto \nu \cdot \frac{u'^2}{\epsilon} \propto \nu \cdot \frac{k}{\epsilon}$$

Microscale:

$$\eta \approx \left(\frac{\nu^3}{\epsilon}\right)^{1/4} \approx L_t/\text{Re}_t^{3/4} \quad \tau_\eta \approx \left(\frac{\nu}{\epsilon}\right)^{1/2} \approx \tau_{L_t}/\text{Re}_t^{1/2}$$

$$u_\eta \approx (\nu \cdot \epsilon)^{1/4} \approx u'/\text{Re}_t^{1/4}$$

Turbulent Reynolds number:

$$\text{Re}_t = \frac{u' \cdot L_t}{\nu}$$

Turbulent Damköhler number:

$$\text{Da} = \frac{\tau_{L_t}}{\tau_c} \approx \frac{L_t/u'}{\delta_l/s_l}$$

Karlovitz number:

$$\text{Ka} = \frac{\tau_c}{\tau_\eta} \approx \frac{\delta_l/s_l}{\eta/u_\eta} \propto \frac{\tau_c}{\tau_\lambda} \approx \frac{\delta_l/s_l}{\lambda/u'}$$

$$\text{Ka} = \frac{\tau_c}{\tau_s} = \frac{\delta_l/s_l}{A_{\text{flame}}/(dA_{\text{flame}}/dt)}$$

APPENDIX B

Evaluation of NO From Strained Flames

In order to separate the NO generated in a strained counterflow flame of reactants and products from that originating from the product inflow, two computations are made for the flame under consideration. In the first run products with a reasonable NO content (e.g., that of an unstrained flame) are specified, whereas in the second run the products are free of NO. As a result two curves

$$\text{NO}_{\text{tot}} = f\left(\frac{T_{ad} - T}{T_{ad} - T_{in}}\right)$$

and

$$\text{NO}_{\text{reactants}} = f\left(\frac{T_{ad} - T}{T_{ad} - T_{in}}\right)$$

are obtained. The difference between the two curves is due to the transport from the product inlet:

$$\text{NO}_{\text{products}} = \text{NO}_{\text{tot}} - \text{NO}_{\text{reactants}}$$

$\text{NO}_{\text{products}}$ can serve as a "tracer" for the diffusion of products toward the reactants, since the diffusivity of NO is similar to the diffusivity of the products. As a consequence, the concentration of products from the product inlet diffusing toward the reactants can be found:

$$X_{\text{products}} = K_{\text{NO}} \cdot \frac{\text{NO}_{\text{products}}}{\text{NO}_{\text{productsinlet}}}$$

K_{NO} represents the thermal NO formation of the products on their way from the inlet toward the reactants. If thermal NO formation is neglected, K_{NO} is set to unity.

Since the products from the combustion of the reactants are diluted with products from the product inlet, the NO concentration is finally normalized:

$$X_{\text{reactants}} = 1 - X_{\text{products}}$$

$$\text{NO}_{\text{reactants,corrected}} = \text{NO}_{\text{reactants}}/X_{\text{reactants}}$$